Continuous Curvature Control of Mobile Robots with Constrained Kinematics ⋆

Vicent Girbés, Leopoldo Armesto and Josep Tornero *

* *Research Institute of Design and Manufacturing at Universidad Politécnica de Valencia, C/ Camino de Vera, 46022, Valencia, Spain (e-mail: {vigirjua,leoaran,jtornero}@upvnet.upv.es).*

Abstract The main contribution of the paper is to provide a method to generate continuous curvature paths in order to perform the kinematic control of a wheeled mobile robot, based on combinations of clothoids, line segments and circular arcs. Higher benefits on comfort and safety can be obtained when generating continuous curvature paths. Wheeled mobile robots following a path with continuous curvature may also get benefit on wheels slippage reduction and low odometry errors, since transitions are softer with constant curvature rates. For that purpose, a general continuous curvature path is derived in order to solve problems with different complexity such as line following problem, path tracking , lane changing and overtaking. Generated paths take into account lower and upper bounds of sharpness and curvature simultaneously, while it is not the case of many kinematic controllers. The proposed kinematic controller determines a whole path to reach a target configuration and it is applied during until the next kinematic control period.

Keywords: **Mobile robots, Automated guided vehicles, Trajectory planning, Path planning, Kinematic Control.**

1. INTRODUCTION

It is well known that comfortability and safety increase when generating continuous curvature paths and trajectories. These aspects become crucial in transporting people or dangerous goods. Wheeled mobile robots following a path with continuous curvature may also get benefit on wheels slippage reduction and low odometry errors, since transitions are softer with constant curvature rates. However, all these aspects have shown little attention and most of well known path planners or kinematic controllers do not take continuous curvature path generation into account.

In recent years many researchers have used clothoids because of their interesting geometric properties and their benefits in comfort and safety. In mobile robotics, clothoids have been used to generate trajectories in navigation problems such as: obstacle avoidance Montes and Tornero (2004), overtaking and lane changing Papadimitriou and Tomizuka (2003), Montes and Tornero (2007), Wilde (2009), parking Laumond et al. (1994), K.Jiang et al. (1999), Gracia and Tornero (2003), among others. In addition to this, clothoids are commonly used in highway design del Corral (2001) and coasters Weiss (1998). Road identification and modeling based on vision systems can be also carried out with clothoids Corridori and Zanin (2004); Manz et al. (2010). See Annex A for a clothoid property summary.

⋆ This work was supported by Generalitat Valenciana (VALi+d Program and PROMETEO), PISALA Project (Universidad Politécnica de Valencia) and DIVISAMOS funded by Spanish Government.

In order to generate continuous curvature paths, most of researchers have used clothoids as transitions curves between lines segments and circular segments and their combinations Iijima et al. (1981); Kanayama and Miyake (1985); Scheuer and Fraichard (1996, 1997a,b). Clothoids are convenient because they provide better comfort (by increase gradually the centrifugal), desirable arrangement for superelevation and satisfactory road appearance. The Standards usually stablish upper bounds on clothoid sharpness based on these three criteria. In addition to this, some authors, see Marchionna and Perco (2007) and the references therein, have shown the inconvenience of using too large clothoid segments since they can have a potentially negative effect on driver's curve perception and safety. As a consequence, some authors suggest lower bound on the clothoid sharpness. Moreover, mechanical constraints on orientable wheels must be also taking into account when generating a path tracking real vehicle which implies a boundary on the maximum allowed curvature.

In Scheuer and Fraichard (1996), Elementary paths were first introduced, a combination of two symmetrical clothoids with the same homotetical factor. These ideas were extended in Scheuer and Fraichard (1997a), by introducing the concept of BiElementary paths, combinations of two Elementary paths. In BiElementary paths the initial and final configurations are not necessary symmetric, but the loci of the intermediate configuration is restricted to a circle with specific orientations to ensure that each Elementary path contain symmetrical clothoids. Obviously, the solution space is significantly limited in those cases and Elementary and BiElementary paths might not be appropriate to solve generic problems.

Dubin's curves were the inspiration in Scheuer and Fraichard (1997b) to create the SCC-paths (single continuous curvature paths) and thus simplify the problem of finding optimal path. Each path is defined as the combination of a maximum of 7 parts between clothoids, circular arcs and line segments. In Scheuer and Xie (1999) a non-holonomic robot without curvature constraints was used to design a generic planner by combining clothoids and anti-clothoids segments. In Reeds and Shepp (1990) RS paths were introduced, and in Fraichard and Desvigne (1999) were used to create the CC paths that ensure continuity, by replacing circular arcs to the called CC-turns. In Fraichard and Ahuactzin (2001) generically global planner continuous curvature paths for vehicles is described. It combines existing systems based on collision avoidance introducing clothoids, lines and circles.

Pure pursuit methods, as Ollero (2001), have been studied intensively in the past and applied on different approaches, covering a wide spectrum of applications such as path tracking, vision-based line following, overtaking maneuvers, lateral tracking, parking, etc. The goal is to determine vehicle's curvature and velocity that can guarantee convergence to a specific path or trajectory. It is quite common in such as methods, to compute goal points based on current vehicles pose relative to the path so they can be applied continuously, by recomputing vehicle's curvature and velocities based on such a relative pose. However, to the authors knowledge, none technique can guaranty continuity on the curvature in order to solve path tracking problems.

The main contribution of the paper is to provide a method to generate continuous curvature trajectories in order to converge to a path, based on combinations of clothoids with line segments and circular arcs. Different kinds of continuous curvature paths have been defined in order to solve problems with different complexity. The simplest one provides continuous curvatures profiles that cannot change from positive to negative or vice versa. More complex solutions provides a general curvature profile that can cope with changes on curvature sign. The type of solutions that we provide get the benefits of higher comfortability and safety. In addition to this, lower and upper bounds on sharpness and curvature are simultaneously taken into account, so every trajectory satisfies those constraints. It is interesting to remark, that the method can be applied off-line or on-line, as a kinematic controller with continuous re-computation of proposed trajectories based on the currents vehicle's position as in pure pursuit framework.

2. CONTINUOUS CURVATURE PATHS GENERATION

2.1 Problem Statement

Definition Let $\mathcal{R}$ a non-holonomic wheeled robot moving on a 2D plane with extended state space $\mathbf{q} = (x, y, \theta, \kappa)^T \in \Re^2 \times \mathcal{S} \times \Re$ containing the robot Cartesian positions x and y, the robot orientation θ and the curvature κ. The kinematic model for $\mathcal{R}$ is:

$$\dot{\mathbf{q}}(t) = \begin{pmatrix} \dot{x}(t) \\ \dot{y}(t) \\ \dot{\theta}(t) \\ \dot{\kappa}(t) \end{pmatrix} = \begin{pmatrix} v(t)\cos(\theta(t)) \\ v(t)\sin(\theta(t)) \\ \kappa(t)v(t) \\ v(t)\sigma(t) \end{pmatrix} \quad (1)$$

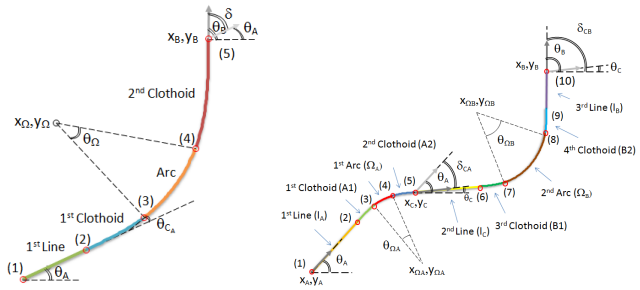

(a) SCC (b) DCC

Figure 1. Variables definition of SCC and DCC paths.

being $v(t)$, $\sigma(t)$ the velocity and sharpness to describe a path respectively. Without loss of generality, the robot configuration is located at the origin $\mathbf{q}_A = (x_A, x_B, \theta_A, \kappa_A)^T$ with $x_A = 0$, $y_A = 0$ and any arbitrary orientation θ_A and curvature κ_A [1].

Definition Let $\mathcal{R}$ a non-holonomic wheeled robot moving on a 2D plane with bounded curvature $\kappa \in [-\kappa_{max}, \kappa_{max}]$ and sharpness $\sigma \in [\sigma_{min}, \sigma_{max}]$. The curvature bounds are due to mechanical constraints of orientable wheels, while sharpness bounds are introduced to increase safety by satisfying the following criteria: comfortability, desirable arrangement for superelevation and road appearance as discussed on Section 1.

The goal is to generate a continuous curvature path $\mathcal{P}$ connecting the actual robot pose $\mathbf{q}_A$ to a target configuration $\mathbf{q}_B = (x_B, y_B, \theta_B, \kappa_B)^T$. Such a target configuration might be determined as usual in motion planning methods such as waypoints of a global path or as in pure pursuit methods by selecting a point at a given distance on the path to track.

2.2 Continuous Curvature Paths Generation

Definition A single continuous curvature path (SCC) is composed by a line segment, a first clothoid, a circle segment (arc) and a second clothoid, as shown in Figure 1(a) with a curvature profile like the one shown in Figure 2(a). These paths are similar to the ones defined in Scheuer and Fraichard (1997b), but clothoids are not neccesarily symmetric. As particular cases the length of line segment and arc can be zero and so only two clothoids are necessary, known as Elementary path Scheuer and Fraichard (1996), which requires that clothoids to be symmetric (with the same sharpness and curvature).

Definition Double continuous curvature paths (DCC) use two single continuous curvature paths (SCC) plus an additional final line segment to provide a set of general solutions. The first SCC path is noted with subindex A and starts at point $\mathbf{q}_A$, while the second SCC path is noted with subindex B finishing at point $\mathbf{q}_B$. The configuration joining both SCC paths is $\mathbf{q}_C = (x_C, y_C, \theta_C, \kappa_C)^T$, with $\kappa_C = 0$. Figure 1(b) shows an example of a DCC path together with the curvature profile in Figure 2(b). It can be appreciated that in that case, we need to generate four clothoids named as $A1$, $A2$, $B1$ and $B2$, two circular segments Ω_A and Ω_B and two line segments with length l_A,

[1] We will assume at the moment the general case where $\kappa_A = 0$ and give particularize the where where $\kappa_A \neq 0$ later on.

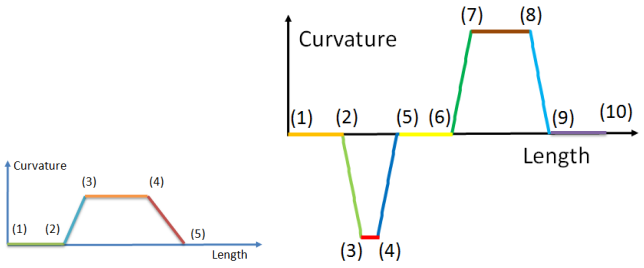

(a) SCC (b) DCC

Figure 2. Curvature Profile of SCC and DCC paths.

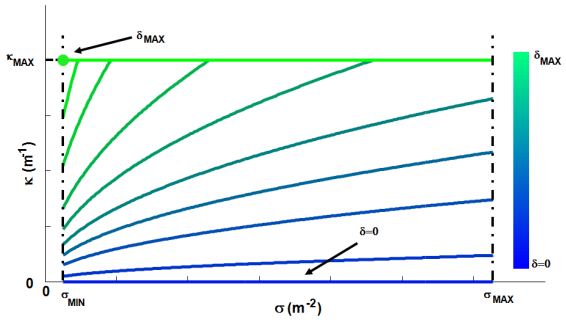

Figure 3. Curvature curve selection for different values of sigma.

l_B and l_C to properly guarantee the appropriate changes on the curvature. Particular solutions can be derived using only four clothoids, obtaining similar solutions of BiElementary path Scheuer and Fraichard (1997a). However, it is interesting to remark the generalization of the formulation provided in this section will allow us to generate a wide spectrum of possible paths with clothoids with different sharpness that can be indistinctly combined.

Let's assume that the sharpness of the four clothoids is given by:

$$\sigma_{C_{A1}} = \alpha_{A1}(\sigma_{max} - \sigma_{min}) + \sigma_{min} \quad (2)$$
$$\sigma_{C_{A2}} = \alpha_{A2}(\sigma_{max} - \sigma_{min}) + \sigma_{min} \quad (3)$$
$$\sigma_{C_{B1}} = \alpha_{B1}(\sigma_{max} - \sigma_{min}) + \sigma_{min} \quad (4)$$
$$\sigma_{C_{B2}} = \alpha_{B2}(\sigma_{max} - \sigma_{min}) + \sigma_{min} \quad (5)$$

being $\alpha_{A1} \in [0,1]$, $\alpha_{A2} \in [0,1]$, $\alpha_{B1} \in [0,1]$ and $\alpha_{B2} \in [0,1]$ design parameters to be determined.

The maximum curvature of each clothoid is:

$$\kappa_{C_{A1}} = \kappa_{C_{A2}} = \min\{\sqrt{\sigma_{C_{A1}}\delta_A}, \sqrt{\sigma_{C_{A2}}\delta_A}, \kappa_{max}\} \quad (6)$$
$$\kappa_{C_{B1}} = \kappa_{C_{B2}} = \min\{\sqrt{\sigma_{C_{B1}}\delta_B}, \sqrt{\sigma_{C_{B2}}\delta_B}, \kappa_{max}\} \quad (7)$$

being $\delta_A = |\theta_A - \theta_C|$ and $\delta_B = |\theta_B - \theta_C|$ the deflection angles between configurations $\angle(\mathbf{q}_A, \mathbf{q}_C)$ and $\angle(\mathbf{q}_C, \mathbf{q}_B)$. Thus, depending on the selected clothoid parameter and deflection angle, we obtain a family of curvature curves as shown in Figure 3.

It can be shown that, the arc of the first circle has zero length if $\sqrt{\sigma_{C_{A1}}\delta} = \sqrt{\sigma_{C_{A2}}\delta_A} < \kappa_{max}$, otherwise, the center of the circle with radius $r_{\Omega_A} = \kappa_{C_{A1}}^{-1}$ whose frame is located at the origin of the first clothoid is:

$$x_{\Omega_A} = x_{C_{A1}} - r_{\Omega_A}\sin\theta_{C_{A1}} \quad (8)$$
$$y_{\Omega_A} = y_{C_{A1}} + r_{\Omega_A}\cos\theta_{C_{A1}} \quad (9)$$

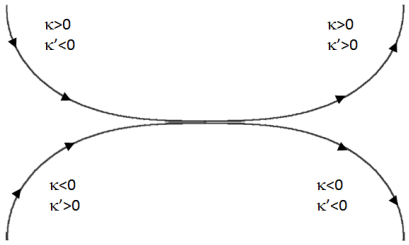

Figure 4. Clothoid paths defined in four quadrants.

with radius $r_{\Omega_A} = \kappa_{C_{A1}}^{-1}$, $r_{\Omega_B} = \kappa_{C_{B1}}^{-1}$ and arc angle $\theta_{\Omega_A} = \theta_C - \theta_A - \theta_{C_{A1}} - \theta_{C_{A2}}$, being $\mathbf{q}_{C_{A1}} = (x_{C_{A1}}, y_{C_{A1}}, \theta_{C_{A1}}, \kappa_{C_{A1}})^T$ the final point of the first clothoid given by Fresnel integrals (see Appendix A:

$$x_{C_{A1}} = \pm\sqrt{\frac{\pi}{\sigma_{C_{A1}}}}\int_0^{\gamma_{C_{A1}}} \cos\frac{\pi}{2}\xi^2 d\xi \quad (10)$$
$$y_{C_{A1}} = \pm\sqrt{\frac{\pi}{\sigma_{C_{A1}}}}\int_0^{\gamma_{C_{A1}}} \sin\frac{\pi}{2}\xi^2 d\xi \quad (11)$$
$$\theta_{C_{A1}} = \pm\frac{\kappa_{C_{A1}}^2}{2\sigma_{C_{A1}}} \quad (12)$$

with $\gamma_{C_{A1}} = \sqrt{\frac{\kappa_{C_{A1}}^2}{\pi\sigma_{C_{A1}}}}$. Eqs. (10) and (11) indicate that any clothoidal combination is possible (on each quadrant) and its sign depends on the conditions that we need positive/negative curvature and positive/negative curvature rate, as shown in Figure 4. The configurations for the second $\mathbf{q}_{C_{A2}}$, third $\mathbf{q}_{C_{B1}}$ and fourth $\mathbf{q}_{C_{B2}}$ clothoids can be similarly defined as well as the center of second circle segment, whose arc angle $\theta_{\Omega_B} = \theta_B - \theta_C - \theta_{C_{B1}} - \theta_{C_{B2}}$ with radius $r_{\Omega_B} = \kappa_{C_{B1}}^{-1}$.

The intermediate configuration $\mathbf{q}_C$ depends on the selected values α_{A1} and α_{A2} for each clothoid as well as selected values for l_A and θ_C, while the remainder of variables will be computed upon those values:

$$\mathbf{q}_C = \underbrace{\begin{pmatrix} x_A \\ y_A \\ \theta_A \\ \kappa_A \end{pmatrix}}_{\text{origin } (\mathbf{q}_A)} + \underbrace{\begin{pmatrix} l_A\cos\theta_A \\ l_A\sin\theta_A \\ 0 \\ 0 \end{pmatrix}}_{1^{\text{st}} \text{ line segment } (l_A)} + \underbrace{\begin{pmatrix} \mathbf{R}(\theta_A)\begin{bmatrix} x_{C_{A1}} \\ y_{C_{A1}} \end{bmatrix} \\ -\theta_{C_{A1}} \\ -\kappa_{C_{A1}} \end{pmatrix}}_{1^{\text{st}} \text{ clothoid } (A1)} + \underbrace{\begin{pmatrix} r_{\Omega_A}\mathbf{R}(\theta_A - \theta_{C_{A1}})\begin{bmatrix} \sin\theta_{\Omega_A} \\ \cos\theta_{\Omega_A} - 1 \end{bmatrix} \\ -\theta_{\Omega_A} \\ 0 \end{pmatrix}}_{\text{arc } (\Omega_A)} + \underbrace{\begin{pmatrix} \mathbf{R}(\theta_C)\begin{bmatrix} x_{C_{A2}} \\ y_{C_{A2}} \end{bmatrix} \\ -\theta_{C_{A2}} \\ \kappa_{C_{A2}} \end{pmatrix}}_{2^{\text{nd}} \text{ clothoid } (A2)} \quad (13)$$

On the other hand, the final configuration $\mathbf{q}_B$ depends on the selected values α_{B1} and α_{B2} for each clothoid and l_C, θ_C and l_B, while the remainder of variables can be easily determined:

$$\mathbf{q}_B = \underbrace{\begin{pmatrix} x_C \\ y_C \\ \theta_C \\ \kappa_C \end{pmatrix}}_{\text{mid conf. } (\mathbf{q}_C)} + \underbrace{\begin{pmatrix} l_C \cos\theta_C \\ l_C \sin\theta_C \\ 0 \\ 0 \end{pmatrix}}_{2^{\text{nd}} \text{ line segment } (l_C)} + \underbrace{\begin{pmatrix} l_B \cos\theta_B \\ l_B \sin\theta_B \\ 0 \\ 0 \end{pmatrix}}_{3^{\text{rd}} \text{ line segment } (l_B)} + \underbrace{\begin{pmatrix} \mathbf{R}(\theta_C)\begin{bmatrix} x_{C_{B1}} \\ y_{C_{B1}} \end{bmatrix} \\ \theta_{C_{B1}} \\ \kappa_{C_{B1}} \end{pmatrix}}_{3^{\text{rd}} \text{ clothoid } (B1)} + \underbrace{\begin{pmatrix} \mathbf{R}(\theta_B)\begin{bmatrix} x_{C_{B2}} \\ -y_{C_{B2}} \end{bmatrix} \\ \theta_{C_{B2}} \\ -\kappa_{C_{B2}} \end{pmatrix}}_{4^{\text{th}} \text{ clothoid } (B2)} + \underbrace{\begin{pmatrix} r_{\Omega_B}\mathbf{R}(\theta_C + \theta_{C_{B1}})\begin{bmatrix} \sin\theta_{\Omega_B} \\ 1-\cos\theta_{\Omega_B} \end{bmatrix} \\ \theta_{\Omega_B} \\ 0 \end{pmatrix}}_{\text{arc } (\Omega_B)} \tag{14}$$

Equations (13) and (14) have been formulated for the case for curvature profiles like those shown in Figure 2(b). They can be generalized to cases where the sign of curvature doesn't change even with four clothoids.

In order to reach the target configuration $\mathbf{q}_B$, we must determine appropriate values for l_A, l_B, l_C and θ_C. With these parameters, we can reach a specific position x_B and y_B, while the appropriate orientation θ_B will be compensated with circular arcs and clothoids. This implies to solve the following equations:

$$X(\theta_C) = l_A \cos\theta_A + l_B \cos\theta_B + l_C \cos\theta_C \tag{15}$$

$$Y(\theta_C) = l_A \sin\theta_A + l_B \sin\theta_B + l_C \sin\theta_C \tag{16}$$

where the terms $X(\theta_C)$ and $Y(\theta_C)$ represent all the terms of equations (13) and (14) but the three line segments, which have been explicitly stated apart here:

$$\begin{bmatrix} X(\theta_C) \\ Y(\theta_C) \end{bmatrix} = \mathbf{q}_B - \mathbf{q}_A - A1 - \Omega_A - A2 - B1 - \Omega_B - B2 \tag{17}$$

An heuristic criteria to determine l_A, l_B, l_C and θ_C is to minimize the length of the overall path while satisfying equations (13) and (14), thus optimal intermediate orientation is:

$$\theta_C^* = \arg\min_{\theta_C} L = l_A + l_{A1} + l_{\Omega_A} + l_{A2} + l_C + l_{B1} + l_{\Omega_B} + l_{B2} + l_B \tag{18}$$

subject to (17), where length of clothoids are obtained form properties stated in Annex A:

$$l_{A1} = \kappa_{A1}(\theta_C)\sigma_{A1}^{-1},\ l_{A2} = \kappa_{A2}(\theta_C)\sigma_{A2}^{-1} \tag{19}$$

$$l_{B1} = \kappa_{B1}(\theta_C)\sigma_{B1}^{-1},\ l_{B2} = \kappa_{B2}(\theta_C)\sigma_{B2}^{-1} \tag{20}$$

$$l_{\Omega_A} = \Omega_A(\theta_C)\kappa_{A1}^{-1}(\theta_C),\ l_{\Omega_B} = \Omega_B(\theta_C)\kappa_{B1}^{-1}(\theta_C) \tag{21}$$

In order to solve this problem, we can force any of the line segments to be zero and then solve the minimization problem. In general, we will be interested in $l_B = 0$ if $\theta_C \neq \theta_A$. Otherwise we have a singular solution that can be avoided by forcing $l_C = 0$ if $\theta_A \neq \theta_B$. If $\theta_A = \theta_B = \theta_C$, then we can not provide a valid solution for such value of θ_C and therefore path length is set to $L = \infty$ to discard these solutions during the minimization step.

On the other hand, in order to extend the scope we need to consider the case when the actual vehicle's curvature is not zero. In that case, we assume that vehicle is indeed located on a given point of the first clothoid A1 of the DCC path, whose origin has to be determined. Also, the curvature of the final configuration point might be distinct from zero and therefore the origin (or terminal point) of that clothoid must be also determined. Since clothoid segments are known a priori, we can compute the points $x_{C_{A1},s}$, $y_{C_{A1},s}$, $x_{C_{B2},e}$ and $y_{C_{B2},e}$ at which their curvatures are respectively $\kappa_{C_{A1},s}$ and $\kappa_{C_{B2},e}$, and obtain their tangent angles $\theta_{C_{A1},s}$ and $\theta_{C_{B2},e}$. The origin of the first and fourth clothoids can be then computed as follows:

$$\mathbf{q'}_A = \begin{pmatrix} x(t) \\ y(t) \end{pmatrix} + \begin{pmatrix} \mathbf{R}(\theta \pm \theta_{C_{A1},s})\begin{bmatrix} \pm x_{C_{A1},s} \\ \pm y_{C_{A1},s} \end{bmatrix} \\ \theta(t) \pm \theta_{C_{A1},s} \\ \kappa_{C_{A1},s} \end{pmatrix} \tag{22}$$

$$\mathbf{q'}_B = \begin{pmatrix} x_B \\ y_B \end{pmatrix} + \begin{pmatrix} \mathbf{R}(\theta_B \pm \theta_{C_{B2},e})\begin{bmatrix} \pm x_{C_{B2},e} \\ \pm y_{C_{B2},e} \end{bmatrix} \\ \theta_B \pm \theta_{C_{B2},e} \\ \kappa_{C_{B2},e} \end{pmatrix} \tag{23}$$

where x, y and θ is the actual vehicle pose and $\mathbf{q'}_A$ and $\mathbf{q'}_B$ are the origins of the clothoids that should replace $\mathbf{q}_A$ and $\mathbf{q}_B$ in Equations 13 and 14.

In that case, when $\kappa_{C_{A1},s} \neq 0$, the length of first and third line segments are set to $l_A = 0$ and $l_B = 0$, while the middle segment length of the second line segment and its orientation can be numerically determined using the fixed-point method from Equations 15 and 16:

$$\theta_C = \arctan\frac{Y(\theta_C)}{X(\theta_C)} \tag{24}$$

2.3 Kinematic Control With Continuous Curvature Paths

Once the DCC path has been computed for the actual vehicle's position and for a given target point, we apply curvature and sharpness profiles during a certain amount of time T, being T the kinematic control period. Therefore, only the first T seconds of the computed trajectory will be taken into account until next control period and the remainder of the trajectory is not used for immediate control. However, we need to compute the whole trajectory since the solution is highly coupled and small changes on the solutions will affect the overall shape of the DCC path.

In pure pursuit methods, we determine a target configuration by finding a point that is at least separated a given distance D from the actual robot pose, satisfying specific application conditions (in order to discard multiple solutions). These ideas have been applied to solve the line following problem as well as vehicle lane change or overtakes. It is out of the scope of the paper to detect conditions when is more appropriate to perform a lane change or an overtake, duration of the maneuver, vehicle speed, etc.

In that sense, in Figure 5 there are several examples of line following paths based on pure pursuit methods with different initial configurations and sharpness, with $D =$ 10m. Based on the initial orientation four different typical paths are obtained which show the flexibility of our path generation method and its line convergence properties. In addition, for each case, sharpness, curvature and steering angle are also depicted in Figure 6 to provide a better insight about the kind of actions applied, where it can be appreciated continuous curvature profiles as claimed.

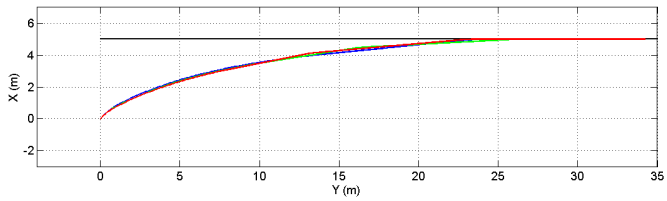

(a) Path with $\theta_A = 45^o$

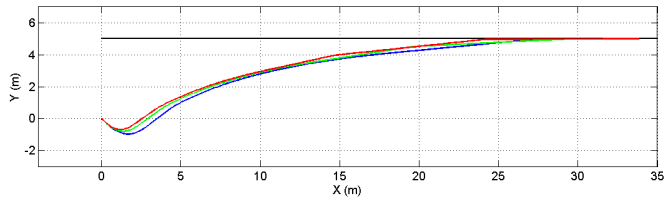

(b) Path with $\theta_A = 135^o$

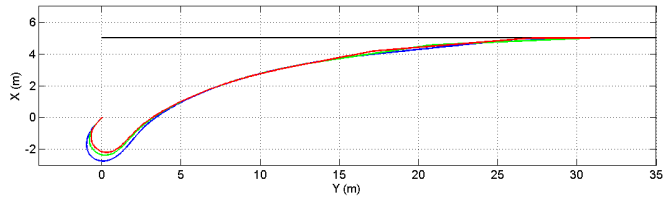

(c) Path with $\theta_A = 225^o$

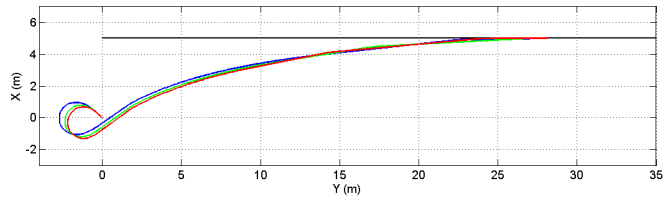

(d) Path with $\theta_A = 315^o$

Figure 5. Examples of line following with different initial configurations and sharpness. Plot colors with increasing sharpness: red, green and blue.

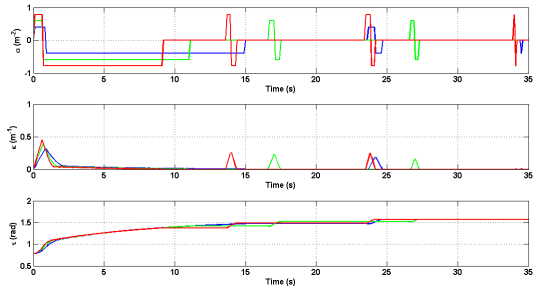

(a) Signals with $\theta_A = 45^o$

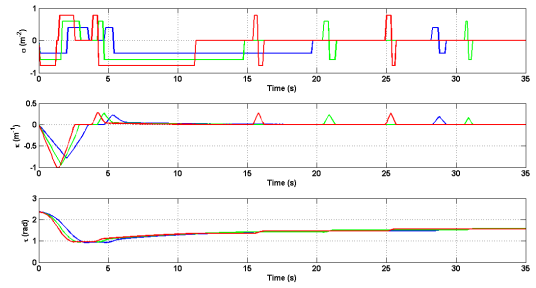

(b) Signals with $\theta_A = 135^o$

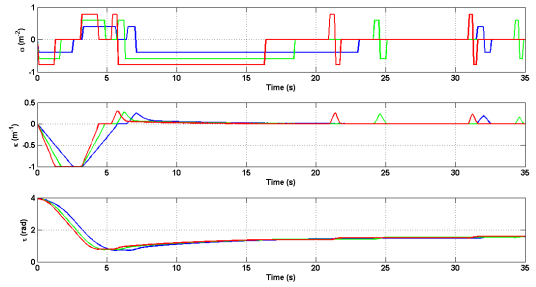

(c) Signals with $\theta_A = 225^o$

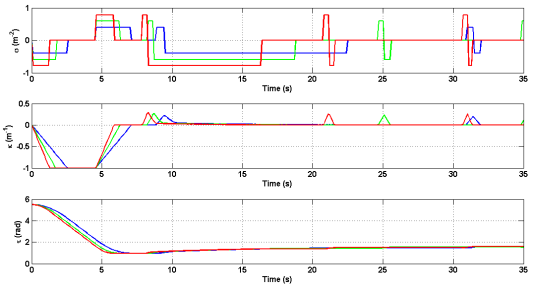

(d) Signals with $\theta_A = 315^o$

Figure 6. Signal profiles of line following examples of Figure 5. Signal subplots are sharpness (σ $[m^{-2}]$), curvature (κ $[m^{-1}]$) and tangent angle (τ $[rd]$).

The sharpness is indeed the curvature derivative and it is not necessary to be continuous. It is interesting to remark that paths with different sharpness have been considered for each case, although there are no significant differences between of the resulting vehicle's trace. The ideas of line following can be extended to generate the trajectories usually required in standard driving. In particular, Figure 7 shows simplistic examples of a conventional lane changing and a vehicle overtaking another vehicle.

On the other hand, the kinematic controller can also be used in combination with path planning methods that provide a set of waypoints. Again, it is out of the scope of the paper to determine such waypoints, but we are interested in performing low level kinematic control to reach all of them. For that purpose, we set as target configuration every waypoint with null curvature and orientation pointing to the next waypoint. Other approach is to define line segments between waypoints and follow them using pure pursuit methods as in previous examples. By doing this, waypoints are approximated by smooth paths satisfying curvature and sharpness constraints. Figure 8 describes an example of the path computed based on just 5 waypoints.

3. CONCLUSIONS

This paper describes a method for generating continuous curvature paths subject to constraints on curve sharpness and maximum curvature. The paper first describes Single Continuous Curvature (SCC) paths, which consist of a line segment, a circular arc segment and two transition curves based on clothoids in order to guarantee a continuous curvature profile. SCC paths are extended to Double Continuous Curvature paths (DCC), which provide a complete solution to include curvature profiles with positive and negative curvatures. It has been shown that SCC and DCC paths can be applied to solve path tracking problem, where the DCC paths can cope with any general configuration and can be easily adapted path tracking based on pure-

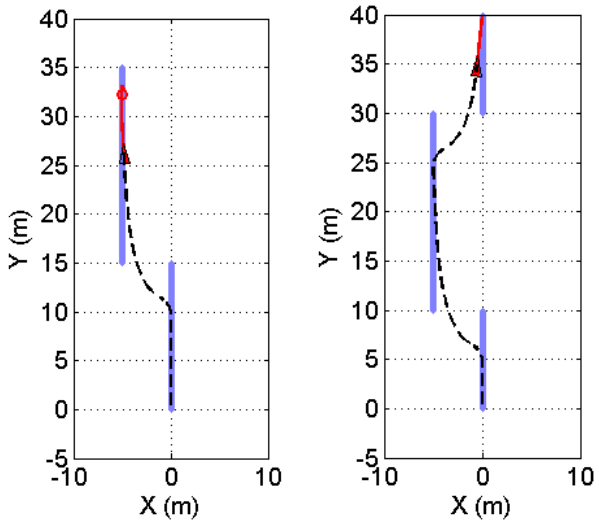

(a) Lane Change (b) Overtaking

Figure 7. Example of lane change and overtaking.

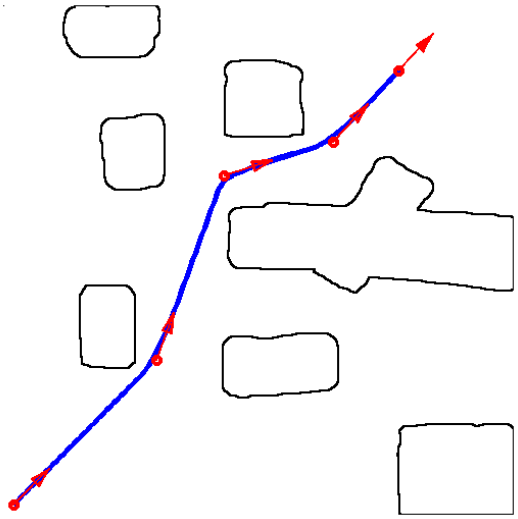

Figure 8. Example of path planning.

pursuit methods or combined with standard path planning methods. We have shown through several simulations that the proposed kinematic controller can be used in line following problems, general path tracking based on waypoints and also in particular cases such as lane changing or overtaking.

Wheeled mobile robots may also get benefit on wheels slippage reduction and low odometry errors, with softer transitions and constant curvature rates when the proposed kinematic controller is used. All these aspects become crucial in transporting people or dangerous goods providing higher comfortability and safety.

REFERENCES

Corridori, C. and Zanin, M. (2004). High curvature two-clothoid road model estimation. In *Intelllgenl Trsnsportation Systems Conference*.

del Corral, I. (2001). *Topografía de obras*. Edicions UPC.

Fraichard and Ahuactzin (2001). Smooth path planning for cars. In *Int. Conference on Robotics and Automation*.

Fraichard, S. and Desvigne (1999). Form reeds and sepp's to continuous curvature paths. In *Int. Conference on Advanced Robotics*.

Gracia, L. and Tornero, J. (2003). Geometric parallel parking planner for car-like vehicles. In *Int. Industrial Simulation Conference*.

Iijima, J., Kanayama, Y., and Yuta, S.i. (1981). A locomotion control system for mobile robots. In *IJCAI'81: Proceedings of the 7th international joint conference on Artificial intelligence*, 779–784. Morgan Kaufmann Publishers Inc., San Francisco, CA, USA.

Kanayama, Y. and Miyake, N. (1985). Trajectory generation for mobile robots. In *Int. Symp. on Robotic Research*.

K.Jiang, D.Z.Zhang, and L.D.Seneviratne (1999). A parallel parking system for a car-like robot with sensor guidance. *Proceedings of the Institution of Mechanical Engineers, Part C: Journal of Mechanical Engineering Science*, 213(6), 591–600. doi:10.1243/0954406991522527.

Laumond, J.P., Jacobs, P., Taix, M., and Murray, R. (1994). A motion planner for nonholonomic mobile robots. *Robotics and Automation, IEEE Transactions on*, 10(5), 577 –593. doi:10.1109/70.326564.

Manz, M., von Hundelshausen, F., and Wuensche, H. (2010). A hybrid estimation approach for autonomous dirt road following using multiple clothoid segments. In *Int. Conference on Robotics and Automation*.

Marchionna, A. and Perco, P. (2007). A proposal to update the clothoid parameter limiting criteria of the italian standard. In *4th International Società Italiana Infrastrutture Viarie Congress*.

Montes, N. and Tornero, J. (2004). Lane changing using s-series clothoidal approximation and dual-rate based on bezier points to controlling vehicle. In *Int. Conference on Systems Theory and Scientific Computation*, 1–6. World Scientific and Engineering Academy and Society (WSEAS), Stevens Point, Wisconsin, USA.

Montes, N. and Tornero, J. (2007). Trajectory generation based on rational bezier curves as clothoids. In *Intelligent Vehicles Symposium*.

Ollero, A. (2001). *Robótica. Manipuladores y robots móviles*. Marcombo, S.A., Barcelona.

Papadimitriou, I. and Tomizuka, M. (2003). Fast lane changing computations using polinomials. In *American Control Conference*.

Reeds, J. and Shepp, L. (1990). Optimal paths for a car that goes both forwards and backwards. *Pacific Journal of Mathematics*, 145, 367–393.

Scheuer, A. and Fraichard, T. (1996). Planning continuous-curvature paths for car-like robots. In *Int. Conf. on Intelligent Robots and Systems*.

Scheuer, A. and Fraichard, T. (1997a). Collision-free and continuous-curvature path planning for car-like robots. In *Int. Conf. on Robotics and Automation*.

Scheuer, A. and Fraichard, T. (1997b). Continuous-curvature path planning for multiple car-like vehicle. In *Int. Conf. on Intelligent Robots and Systems*.

Scheuer, A. and Xie (1999). Continuous-curvature trajectory planning for maneuverable non-holonomic robots. In *Int. Conf. on Intelligent Robots and Systems*.

Weiss, D.L. (1998). *Dynamic Simulation and Analysis of Roller Coasters*. Ph.D. thesis, University of California, Davis.

Wilde, D.K. (2009). Computing lothoid segments for trajectory generation. In *Int. Conference on Robotics and Automation*.

Appendix A. SUMMARY OF CLOTHOIDS

Definition Cornu's Spiral or Clothoid is defined by the Fresnel integrals in $\Re^2$ as follows:

$$\mathcal{C}(\gamma) = \begin{bmatrix} C_x(\gamma) \\ C_y(\gamma) \end{bmatrix} = K \begin{bmatrix} \int_0^\gamma \cos \frac{\pi}{2}\xi^2 d\xi \\ \int_0^\gamma \sin \frac{\pi}{2}\xi^2 d\xi \end{bmatrix} \tag{A.1}$$

where K is the Homotetical factor, i.e.: the scale of the spiral, and γ is comprises the integration interval. Unfortunately, there is no closed-form solution to compute Fresnel integrals, however some interesting geometric properties of clothoids can be analytically computed.

Properties Let $\mathcal{C}(\gamma)$ be a clothoid curve, the so called clothoid parameter A and its homotetical factor are related by $K = \sqrt{\pi}A$. The tangent angle τ with respect to the abscissa axis $\mathcal{X}^+$ of $\mathcal{C}(\gamma)$ is $\tau = \frac{\pi}{2}\gamma^2$. The curvature κ and length L of the clothoid $\mathcal{C}(\gamma)$ increase proportionally with γ for a given Homotetical factor, being the expression $\kappa = \pi\frac{\gamma}{K}$ for curvature and $L = K\gamma$ for the length. It is straight forward to see that both, curvature and length are related by the clothoid parameter as $\kappa = \frac{L}{A^2}$, which implies that constant changes on the curvature are proportional to changes on the length of the curve. The sharpness is defined as $\sigma \equiv A^{-2}$ and therefore the higher the clothoid parameter the lower the sharpness and vice versa.